Bioorganic & Medicinal Chemistry 18 (2010) 1910–1917

Contents lists available at ScienceDirect

Bioorganic & Medicinal Chemistry

journal homepage: www.elsevier.com/locate/bmc

Benzyl 1,2,3,5,11,11a-hexahydro-3,3-dimethyl-1-oxo-6*H*-imidazo[3′,4′:1,2]pyridin[3,4-*b*]indole-2-substituted acetates: One-pot-preparation, anti-tumor activity, docking toward DNA and 3D QSAR analysis

Jiawang Liu [a], Ming Zhao [a,*], Keduo Qian [b], Xiaoyi Zhang [a], Kuo-Hsiung Lee [b,*], Jianhui Wu [a], Yi-Nan Liu [b], Shiqi Peng [a,*]

[a] College of Pharmaceutical Sciences, Capital Medical University, Beijing 100069, PR China
[b] Natural Products Research Laboratories, School of Pharmacy, University of North Carolina, Chapel Hill, NC 27599-7360, USA

ARTICLE INFO

Article history:
Received 1 November 2009
Revised 15 January 2010
Accepted 16 January 2010
Available online 25 January 2010

Keywords:
β-Carboline-3-carboxylic acid
Anti-tumor activity
Neurotoxicity
Organ damage
3D QSAR
Log *P*
Docking

ABSTRACT

To discover the anti-tumoral indoles a series of benzyl 1,2,3,5,11,11a-hexahydro-3,3-dimethyl-1-oxo-6*H*-imidazo[3′,4′:1,2]pyridin[3,4-*b*]indole-2-substituted acetates (**2a–n**) are prepared via one-pot-preparation. The IC_{50} values of **2a–n** in vitro against human lung carcinoma, prostate cancer, nasopharyngeal carcinoma, vincristine-resistant KB subline and human breast carcinoma cells range from 40 nM to 60 μM. On Sarcoma 180 (S180) tumor-bearing mouse model four of them (**2e,g,h,i**) significantly inhibited the tumor growth. At the dose of 0.1 mg/kg the efficacy of the most potent **2h** was equal to that of 1.0 mg/kg of doxorubicin. In contrast to doxorubicin, at 1.0 mg/kg of dose **2e,g,h,i** did not induce the treated S180 mice to have organ atrophy and body emaciation. The healthy mice receiving 10, 100 and 500 mg/kg of **2e,g,h,i** gave no any neurotoxic response. Even up to the dose of 500 mg/kg the healthy mice occurred no death. The interaction of **2a–n** with DNA was confirmed by the fluorescence quenching experiments and automated flexible ligand docking. By 3D QSAR analysis the IC_{50} values of **2a–n** against prostate cancer cells were correlated with the structures and conformations of their side chains. To increase the data related to their physical-chemical properties the experimental Log *P* values were also provided.

1. Introduction

Despite a better understanding of the disease, the advent of modern technology and rationally targeted drugs, the incidence and cure rate of cancer have not improved. In the past decades continuous efforts have been made for discovering of new anti-tumor compounds and a number of substances have been reported. Among the discovered substances β-carboline derivatives have been particularly known possessing diverse action mechanism. β-Carboline derivatives may induce DNA damage,[1] intercalate toward DNA,[2] bind minor groove,[3,4] inhibit DNA synthesis[5] or repair DNA.[6] β-Carboline derivatives are also capable of inducing crossing-over and mitotic gene conversion[7], modulating the extrinsic or death receptor pathway and the intrinsic or mitochondrial pathway[8], as well as target Ras and their signaling pathways.[9] β-Carboline derivatives may also inhibit indoleamine 2,3-dioxygenase,[10] topoisomerase[11–13] and cyclin-dependent kinases.[13,14] Among these action mechanisms intercalation has particular importance in the clinical oncology and some β-carboline derivatives are routinely used.[15,16]

Structurally, β-carboline derivatives with DNA intercalation activities are characterized by a polycyclic aromatic planar pharmacophore capable of stacking between DNA pairs.[17,18] However, DNA intercalation of substituted β-carbolines may result in serious neurotoxicity.[19] Discovering of non-neurotoxic β-carbolines has attracted a lot of interests.[20,21] As part of our ongoing efforts, recently a series of β-carboline-3- carbonylamino acid benzyl ester conjugates were evaluated as potent anticancer agents and substituted benzyl 1,2,3,5,11,11a-hexahydro-3,3-dimethyl-1-oxo-6*H*-imidazo[3′,4′:1,2]pyridin[3,4-*b*]indole-2-acetates were considered P glucose protein (Pgp) inhibitors possessing reversing resistance activity.[22] Afterwards they were found having low neurotoxicity. In this context, in the present paper the in vitro anti-proliferation, in vivo anti-tumor activity, neurotoxicity, organ damage, acute toxicity, 3D QSAR analysis, experimental Log *P* values and intercalating mechanism of β-carboline derivatives, benzyl 1,2,3,5,11,11a-hexahydro-3,3-dimethyl-1-oxo-6*H*-imidazo[3′,4′:1,2]pyridin[3,4-*b*]indole-2-substituted acetates, were investigated.

* Corresponding authors. Tel./fax: +86 10 8391 1528 (S.P.); +86 10 8280 2482 (M.Z).
E-mail addresses: mingzhao@bjmu.edu.cn (M. Zhao), shiqipeng@163.com, sqpeng@bjmu.edu.cn (S. Peng).

0968-0896/$ - see front matter © 2010 Elsevier Ltd. All rights reserved.
doi:10.1016/j.bmc.2010.01.038

2. Results and discussion

2.1. Chemistry

The synthetic route was depicted in Scheme 1. In this one-pot-three-step procedure 3*S*-*N*-Boc-1,2,3,4-tetrahydro-β-carboline-3-carboxylic acid was firstly prepared from the coupling of β-carboline-3-carboxylic acid and Boc-N_3. The coupling product was then amidated with L-amino acid benzylester to gave 3*S*-*N*-Boc-1,2,3,4-tetrahydro-β-carboline-3-carbonyl-L-amino acid benzylester, which was unprotected to remove the Boc group, and treated with acetone and triethylamine to form benzyl 1,2,3,5,11,11a-hexahydro-3,3-dimethyl-1-oxo-6*H*-imidazo[3′,4′:1,2]-pyridin[3,4-*b*]indole- 2-substituted acetates (**2a–n**). The crystals of **2a–n** were collected from methanol in 36–48% total yields. HPLC analysis indicated that the purities of **2a–n** ranged from 98.0% to 98.9%. These data suggest that this one-pot-three-step synthesis is suitable for simply preparing **2a–n**.

2.2. Effects of 2a–n on the proliferation of five human carcinoma cell lines

In the anti-proliferation assays, human lung carcinoma (A549), prostate cancer (PC-3), nasopharyngeal carcinoma (KB), vincristine-resistant KB subline (KB-VIN) and human breast carcinoma (MCF-7) cell lines were exposed to serial concentrations (60, 6, 0.6, 0.06 and 0.006 μM) of **2a–n**, and the sulforhodamine B assays were performed. The IC_{50} values of **2a–n** against these five cell lines are summarized in Table 1. The data indicate that besides **2e,g,h,i,l** highly inhibit the proliferation of A549, PC-3 and MCF-7 cell lines, most of **2a–n** highly inhibit the proliferation of PC-3 cell lines. While **2a–d,f,j,k,m,n** moderately inhibit the proliferation of A549, MCF-7, KB and KB-VIN cell lines. Compounds **2e,g,h,i,l** are the most active compounds in vitro.

2.3. Effect of 2a–n on tumor weights of the treated S180 mice

The in vivo anti-tumor activities of **2a–n** were evaluated on S180 mouse model, while doxorubicin and normal saline (NS) were used as the positive and negative controls, respectively. The data are listed in Table 2. The data indicate that when S180 mice were given a daily ip injection of 0.2 mL of the solution of 1.0 mg/kg of each of **2a–n** in NS for seven consecutive days **2e,g,h,i** significantly inhibit the tumor growth of S180 mice. Excepting **2l**, the in vivo determination matches with the in vitro determination. With regard to the structures of **2a–n** the side chain of **2l** is the longest one. Comparing to the short side chain the long one should be more sensitive to the in vivo metabolism. This may be responsible

Table 1
IC_{50} values of **2a–n** against A549, PC-3, MCF-7, KB and KB-VIN cell lines

Compd	IC_{50} (μM)				
	A549	PC-3	MCF-7	KB	KB-VIN
2a	43.57	10.33	21.11	50.13	50.90
2b	44.94	8.47	33.71	52.00	52.21
2c	30.57	7.06	14.71	41.15	32.48
2d	59.06	47.96	57.00	60.34	55.72
2e	7.92	9.98	10.37	22.48	12.23
2f	35.28	40.57	43.00	46.39	41.12
2g	0.12	0.69	4.44	18.02	8.35
2h	0.39	0.21	4.04	37.59	8.48
2i	0.15	0.04	7.01	36.30	38.62
2j	33.59	35.40	37.04	40.01	37.92
2k	23.27	13.92	19.81	38.24	42.26
2l	8.34	4.24	4.61	32.89	30.55
2m	39.59	16.96	20.17	43.47	50.11
2n	38.42	10.00	20.44	42.10	40.00

Table 2
Effects of **2a–n** on tumor weights of S180 mice[a]

Compd	Tumor weight
NS	1.602 ± 0.391
Doxorubicin	0.817 ± 0.369[b]
2a	2.846 ± 0.330
2b	2.003 ± 0.284
2c	2.050 ± 0.447
2d	1.418 ± 0.075
2e	0.916 ± 0.370[c]
2h	A 0.713 ± 0.310[d]
	B 0.955 ± 0.221[e]
	C 1.244 ± 0.252[f]
2f	1.600 ± 0.352
2g	1.046 ± 0.176[b]
2i	A 0.746 ± 0.313[c]
	B 1.013 ± 0.207[g]
	C 1.305 ± 0.224[h]
2j	1.578 ± 0.498
2k	1.793 ± 0.147
2l	1.613 ± 0.360
2m	1.604 ± 0.295
2n	1.696 ± 0.156

[a] Dose of doxorubicin and **2a–n**: 1.0 mg/kg; dose of **2h-**A, B and C are 1.0, 0.1 and 0.01 mg/kg, respectively; NS = vehicle, $n = 12$, tumor weight is represented by $\bar{x} \pm SD$ g.
[b] Compared to NS $p < 0.01$.
[c] Compared to NS $p < 0.01$, to **2i**-B $p < 0.05$, to doxorubicin $p > 0.05$.
[d] Compared to NS $p < 0.01$, to **2h**-B $p < 0.05$, to doxorubicin $p > 0.05$.
[e] Compared to NS $p < 0.01$, to **2h**-C $p < 0.01$, to doxorubicin $p > 0.05$.
[f] Compared to NS $p < 0.05$.
[g] Compared to NS $p < 0.01$, to **2i**-C $p < 0.05$.
[h] Compared to NS $p < 0.05$.

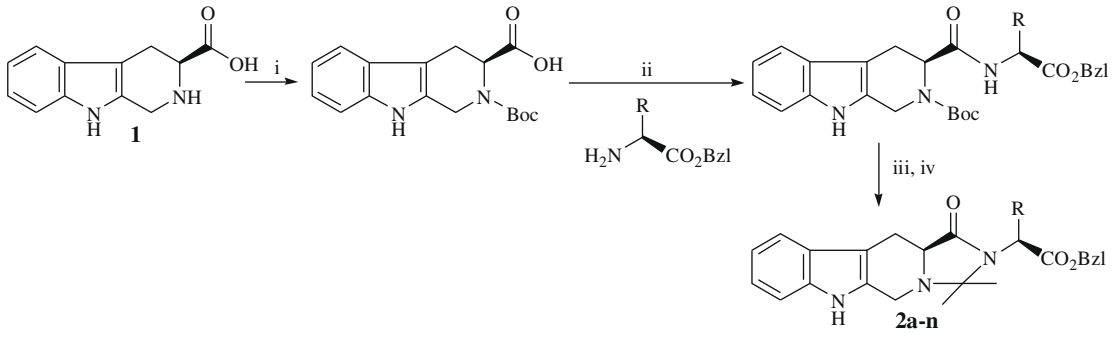

Scheme 1. Synthetic route of benzyl 1,2,3,5,11,11a-hexahydro-3,3-dimethyl-1-oxo-6*H*-imidazo-[3′,4′:1,2]pyridin[3,4-*b*]indole-2-substituted acetates. (i) Boc-N_3, DMF; (ii) DCC, HOBt; (iii) HCl in EtOAc(4 N); (iv) MeOH, acetone, Et_3N. In **2a** R = $CH(CH_3)CH_2CH_3$; **2b** R = $CH(CH_3)_2$; **2c** R = $CH_2CH(CH_3)_2$; **2d** R = CH_3; **2e** R = H; **2f** R = $CH_2C_6H_5$; **2g** R = $CH_2C_6H_4$-OH-p; **2h** R = Indole-3-yl-CH_2; **2i** R = CH_2CO_2Bzl; **2j** R = $CH_2CH_2CO_2Bzl$; **2k** R = CH_2OBzl; **2l** R = $CH_2CH_2CH_2CH_2NHCBz$; **2m** R = CH_2CONH_2; **2n** R = $CH_2CH_2CONH_2$.

for the in vivo data of **2l** mismatch the in vitro data. The data also indicate that the therapeutic potency of **2e,h,i** equals to doxorubicin (tumor weight, 0.817 g). This means **2e,h,i** possess desirable therapeutic efficacy.

The most in vivo active **2h** and **2i** were observed at doses of 1.0, 0.1 and 0.01 mg/kg to produce a possible dose-dependent in vivo anti-tumor response in S180 mice. The data are also listed in Table 2, which demonstrate that the tumor weight of the treated mice is progressively increased with dose decrease. Therefore, these experiments explored that ip injection of **2h** and **2i** exhibited dose-dependent anti-tumor action.

2.4. Organ and body damage of 2e,g,h,i to the treated S180 mice

As one of visible results of chemotherapeutic toxicity related organ damage should be organ atrophy. To evaluate the organ and body damage the organ and body weights of the most potency **2e,g,h,i** treated S180 mice were measured. Twenty-four hours after the last administration the mice were measured for body weights, and then all mice were sacrificed by diethyl ether anesthesia and dissected to immediately obtain and weigh the liver, kidney, brain, spleen, heart and left femur samples (Table 3). It was found that except brain, the weights of the liver, kidney, spleen, heart, left femur and body of doxorubicin receiving S180 mice were significantly lower than that of NS receiving S180 mice. This comparison demonstrates that doxorubicin therapy may induce organ atrophy and body emaciation for S180 mice. While the weights of the liver, kidney, spleen, heart, left femur and body of **2e,g,h,i** receiving S180 mice were not significantly different from that of NS receiving S180 mice. This comparison demonstrates that 2e,**g**,**h**,**i** therapy results no similar side effects to that of doxorubicin.

2.5. Neurotoxic and acute toxicities of 2e,g,h,i receiving healthy mice

Neurotoxic and acute toxicities of the most potent **2e,g,h,i** received healthy mice were assayed by use of a general procedure. It was found that during 7-day observation 10, 100 and 500 mg/kg of **2e,g,h,i** (ip) receiving healthy mice exhibited no any neurotoxic behavior, such as tremor, twitch, jumping, tetanus, as well as supination. On the seventh day the necropsy findings of the mice gave also no apparent changes in their organs. These observations suggest that **2e,g,h,i** should be low toxic agents. Besides, even up to 500 mg/kg of dose the treated healthy mice occurred no death. This observation suggests that the LD_{50} value of **2e,g,h,i** are more than 500 mg/kg. It is generally accepted that most of β-carbolines are strong neurotoxicity and the treated animals have low survival.[22] At the dose of 500 mg/kg the treated mice having high survival and without neurotoxic behavior implies that **2e,-g,h,i** should be promising anti-tumor leads.

2.6. Log *K* of 2a–n

The Log *P* value, defined as the logarithm of the partition coefficient between *n*-octanol and water, is an important parameter to reflect a compound's bioavailability. Meanwhile, it has been widely used as an important molecular descriptor in QSAR such as the classical Hansch approach.[23] It is well known that Log *K* values are highly correlated with the corresponding Log *P* values, and have been generally used to replace the time-consuming Log *P* determination. Therefore, the Log *K* values of **2a–n** provided here could be practically useful.

Each of **2a–n** was dissolved in aqueous methanol (50%) to prepare sample solution (10 μM). The HPLC analysis was carried out on Agilent 1100 series, the column was a reversed-phase C18 column (Agilent Zorbax Extend-C18, 4.6 × 15 mm, 5 μm). After 20 μL of the sample solution was loaded, the column was eluted with 50% solution of MeOH as the mobile phase for 40 min. The flow rate was 1 mL/min. Each of **2a–n** in the sample was monitored with UV detector at 254.8 nm and the retention time (t_R) of the peak was recorded. In the same HPLC conditions the retention time of acetone peak was recorded as t_0. In order to offset the influence of the solvent on the appearance time of the peak of **2a–n**, the appearance time of acetone peak (t_0, 1.591 min) was used as a control. According to the common knowledge that Log *K* is alternative representation of t_R, the Log *K* values of **2a–n** were calculated based on the equation $\text{Log } K = \text{Log}[(t_R - t_0)/t_0]$ and are listed in Table 4.

It was noticed that the Log *K* values of **2a–n** not correlated with the substituent hydrophobicity constant. By using the QSAR module of Cerius[2] the substituent hydrophobicity constant based Log *P* values were calculated and are also displayed in Table 4. To discuss the correlation of the Log *K* value with the experimental Log *P* values the calibration curves of **2a–n** are making. The experimental Log *P* values, the correlation of the Log *K* value with the experimental Log *P* value and the QSAR analysis of the experimental Log *P* value and anti-tumor activity will be reported in a separate paper.

2.7. 3D QSAR equation of 2a–n inhibiting proliferation of PC-3 cell lines

To analyze the relationship of the structures and the anti-tumor activities of **2a–n** the valid 3D QSAR models of Cerius[2] were used. With an assumption that all structures of **2a–n** bind the same site of the receptor with their common hexahydro-3,3-dimethyl-1-oxo-6*H*-imidazo[3′,4′:1,2]pyridin[3,4-*b*]indole ring the maximum common subgraph (MCS) was used.[24] After energy-minimization

Table 3
Body and organ weights of **2e**,**g**,**h**,**i** receiving S180 mice[a]

Compd	Body and organ weight (mean ±SD g)						
	Body	Brain	Heart	Liver	Spleen	Kidney	Femur
NS	33.30 ± 2.32	0.31 ± 0.01	0.17 ± 0.01	2.36 ± 0.20	0.22 ± 0.04	0.23 ± 0.02	0.056 ± 0.006
DXB	27.28 ± 2.40[b]	0.32 ± 0.01	0.15 ± 0.03[c]	2.00 ± 0.25[d]	0.11 ± 0.02[b]	0.19 ± 0.01[e]	0.046 ± 0.003[b]
2e	33.75 ± 1.52	0.30 ± 0.02	0.16 ± 0.02	2.25 ± 0.30	0.24 ± 0.03	0.22 ± 0.02	0.055 ± 0.004
2g	35.85 ± 3.03	0.32 ± 0.01	0.16 ± 0.01	2.35 ± 0.22	0.23 ± 0.02	0.23 ± 0.02	0.056 ± 0.005
2h	32.89 ± 3.79	0.30 ± 0.02	0.17 ± 0.02	2.29 ± 0.25	0.22 ± 0.03	0.21 ± 0.02	0.050 ± 0.003
2i	33.37 ± 2.19	0.31 ± 0.01	0.17 ± 0.03	2.26 ± 0.21	0.24 ± 0.02	0.23 ± 0.01	0.057 ± 0.005

[a] Dose of doxorubicin and **2e**,**g**,**h**,**i**: 1.0 mg/kg, NS = vehicle, $n = 12$.
[b] Compare to NS and **2e**,**g**,**h**,**i** $p < 0.01$.
[c] Compare to NS $p < 0.05$.
[d] Compare to NS and **2g**,**h** $p < 0.01$, to **2e**,**i** $p < 0.05$.
[e] Compare to NS and **2e**,**g**,**h**,**i** $p < 0.05$.

Table 4
Log *K* and Calculated Log *P* values of **2a–n**

Compd	Log *K*	Cal. Log *P*
2a	0.80	2.79
2b	0.73	2.26
2c	0.92	2.79
2d	0.44	1.33
2e	0.32	0.93
2f	1.05	3.05
2g	0.49	2.85
2h	0.81	2.41
2i	0.96	0.30
2j	1.05	0.83
2k	1.02	2.00
2l	0.87	3.15
2m	0.16	−0.105
2n	0.25	−0.522

using the MMFF94 (Merck Molecular Force Field), the Molecular Field Analysis (MFA) was performed for **2a–n** using the QSAR module of Cerius^2.[25] Three probes were chosen to describe **2a–n**. Methyl group was used to account for steric contacts, while proton and hydroxyl ion probes were used to evaluate electrostatic potential fields. The model of MFA of **2a–n** inhibiting the proliferation of PC-3 cell lines in terms of the descriptors proton, methyl and hydroxyl ion was expressed by Eq. 1. The data points (n), correlation coefficient (r) and square correlation coefficient (r^2) of Eq. 1 were 14, 0.996 and 0.991, respectively. The IC_{50} values of **2a–n** and their analogs against the proliferation of PC-3 cell lines can be predicted with Eq. 1. With the predicted IC_{50} values as the ordinate and the experimental IC_{50} values as the abscissa Figure 1 was obtained.

$$\begin{aligned} IC_{50} = {} & 10.26 - 0.30(H^+/478) - 0.9(CH_3/437) \\ & - 0.028(CH_3/783) + 0.46(CH_3/798) - 0.08(CH_3/928) \\ & - 0.46(HO^-/578) - 0.055(HO^-/584) \\ & + 1.25(HO^-/587) - 0.24(HO^-/797) + 0.42(HO^-/885) \\ & - 0.09(HO^-/918) \end{aligned} \quad (1)$$

Eq. 1 contains 1 term from proton descriptor, 4 terms from methyl descriptor and 6 terms from hydroxyl anion descriptor. The term of 0.30 (H^+/478) has negative coefficient, which means that at this position electron-withdrawing group will increase the activity. The term of 0.46 (CH_3/798) has positive coefficient, which means that at this position small group will increase the activity, while terms of 0.9 (CH_3/437), 0.028 (CH_3/783), and 0.08 (CH_3/928) have negative coefficients, which means that at these positions large groups will increase the activity. The terms of 1.25 (HO^-/587) and 0.42 (HO^-/885) have positive coefficients, which means that at these positions hydrogen bond forming groups will decrease the activity, while the terms of 0.46 (HO^-/578), 0.055 (HO^-/584), 0.24 (HO^-/797) and 0.09 (HO^-/918) have negative coefficients, which means that at these positions hydrogen bond forming groups will increase the activity. These structural requirements could be useful for the design of novel compounds.

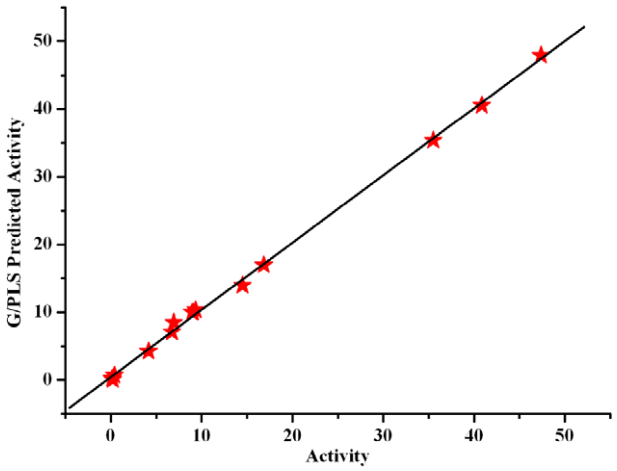

Figure 1. Graph of tested versus predicted activities of **2a–n** inhibiting the proliferation of PC-3 cells.

2.8. Diagrammatic examples of Eq. 1

Figure 2 gives **2h,i** as diagrammatic examples of Eq. 1. Compound **2h** has small group near the region of CH_3/798, as well as hydrogen bond forming groups near the regions of HO^-/578, HO^-/797 and HO^-/918 thus it has high in vitro anti-proliferation activity. Using Eq. 1 the IC_{50} of **2h** was calculated to be 0.14 μM. Compound **2i** has small group near the regions of CH_3/798, as well as a hydrogen bond forming groups near the regions of HO^-/578, HO^-/584, HO^-/797 and HO^-/918, thus it also has high in vitro anti-proliferation activity. Using Eq. 1 the IC_{50} of **2i** was calculated to be 0.22 μM.

Figure 3 gives **2d,f** as diagrammatic examples of Eq. 1. Compound **2d** has electron-releasing group near the region of H^+/478, small groups near the regions of CH_3/437 and CH_3/783, as well as hydrogen bond forming groups near the regions of HO^-/587 and HO^-/885, thus it has low in vitro anti-proliferation activity. Using Eq. 1 the IC_{50} of **2d** was calculated to be 47.3 μM. Compound **2f** has electron-releasing group near the region of H^+/478, small groups near the regions of CH_3/437, CH_3/783 and CH_3/928, as well as a hydrogen bond forming group near the region of HO^-/587, thus it also has low in vitro anti-proliferation activity. Using Eq. 1 the IC_{50} of **2f** was calculated to be 40.9 μM.

2.9. Fluorescence evidence for the interaction of 2h,i with DNA

DNA spectra are widely used to study the interaction of small molecules with DNA. To reveal the possible interaction CT DNA was selected as the model DNA, and the interaction of **2a–n** with DNA was explained by fluorescence tests of the system of CT DNA and the most potent **2h** and **2i**. The effect of CT DNA on the fluorescence intensity of **2h** or **2i** was determined on fluorescence spectroscopy at 300 K. The solution of **2h** or **2i** in PBS (1.0 μM, pH 7.4) was titrated with 10 μL of the solution of CT DNA in PBS at a series of concentrations (0, 9, 18, 27, 36, 45, 54, 63, 72, 81 μM, pH 7.4) to observe the change of the fluorescence intensity on a Shimadzu RF-5310PC spectrofluorometer at a fluorescence excitation wavelength of 245 nm. It was found that CT DNA titration defined a concentration-dependent decrease of fluorescence intensities (fluorescence quenching) of **2h** and **2i**. Figure 4 describes a typical course of the fluorescence quenching, that is, a gradual decrease of the fluorescence intensity of **2h** and **2i** follows a gradual increase of the concentration of CT DNA. When the concentration of CT DNA was increased to 81 μM the fluorescence intensity of **2h** and **2i** was lowered to their minima. The fluorescence quenching of **2h** and **2i** induced by 81 μM of CT DNA was 45.07%. From the courses of the fluorescence quenching a set of slightly bathochromic shift was noticed. This bathochromic shift is considered associating with the decrease in the energy gap between the highest occupied molecular orbital and the lowest occupied molecular orbital occurs in the interaction of **2a–n** with CT DNA.[21,26]

2.10. Docking of 2a–n toward oligoribonucleotides

For the docking investigation of drugs toward DNA 263D (minor/major groove binding), 1NAB-2 (intercalation plus groove binding)

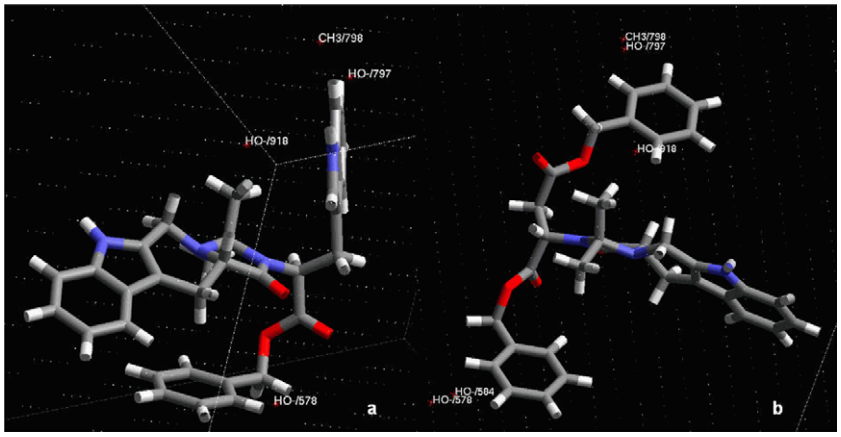

Figure 2. Electrostatic and environments of **2h** (a) and **2i** (b) within the grid with 3D points of Eq. 1.

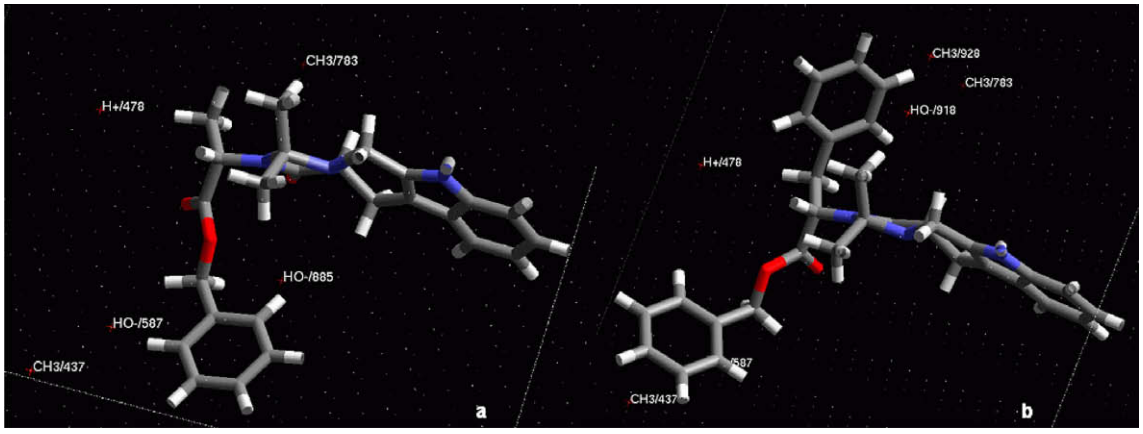

Figure 3. Electrostatic and environments of **2d** (a) and **2f** (b) within the grid with 3D points of Eq. 1.

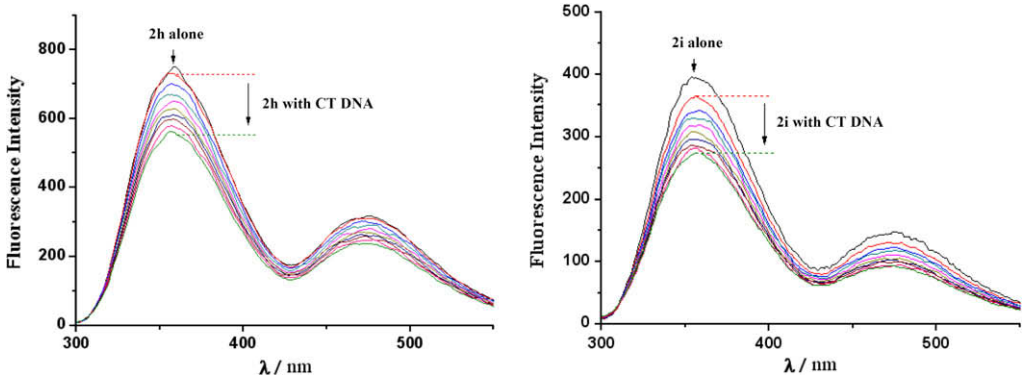

Figure 4. Fluorescent spectra of **2h,i** (concentration 1 μM, pH 7.4, λ_{max} = 254 nm) with serial concentrations (0, 9, 18, 27, 36, 45, 54, 63, 72, 81 μM) of CT DNA in PBS.

and 1NAB-1 (intercalation) have been considered, and the double-stranded oligoribonucleotides d(CGATCG)$_2$ (PDB ID: 1NAB),[27] as well as d(CGCAAATTTGCG)$_2$ (PDB ID: 263D),[28] have been used to simulate DNA. To explore the interaction patterns of **2a–n** with DNA, based on the generalized CHARMm force field in Discovery Studio Modeling 2.1, the automated docking studies were performed. In these studies a standard procedure of the LIGAND-FIT/LIGAND-SCORE was followed. Following the three interaction patterns the final docking energies of **2a–n** were calculated and the data are listed in Table 5.

The final docking energy indicates that though there are three interaction patterns, **2a–n** are able to take two of them only. For instance, **2a–g,m,n** possibly take 1NAB-1 and 263D, **2i–l** possibly take 1NAB-1 and 1NAB-2, while **2h** possibly take 1NAB-2 and 263D. On the other hand, for the most potent **2e**, **2g**, **2h** and **2i** the orders of the final docking energies are 263D < 1NAB-

Table 5
Final docking energy (kcal/mol) of **2a**–**n** toward DNA

Compd	1NAB		263D
	1NAB-1	1NAB-2	
2a	−45.60	—	−68.00
2b	−27.00	—	−53.44
2c	−75.57	—	−60.47
2d	−26.83	—	−20.80
2e	−77.17	—	−118.45
2f	−57.20	—	−3.90
2g	−0.50	—	−104.80
2h	—	−73.12	−44.10
2i	−89.83	−23.13	—
2j	−54.79	−29.18	—
2k	−31.40	−77.64	—
2l	−34.00	−59.63	—
2m	−73.05	—	−43.95
2n	−56.00	—	−33.76

1 < 1NAB-2, 263D < 1NAB-1 < 1NAB-2, 1NAB-2 < 263D < 1NAB-1 and 1NAB-1 < 1NAB-2 < 263D, respectively. This means that **2e**, **2g**, **2h** and **2i** may interact with DNA by selecting 263D, 1NAB-2 and 1NAB-1, respectively. A selective pattern matches the lowest docking energy. To visualize the interaction pattern the graphical descriptions of the selective docking of **2e**,**g**,**h**,**i** toward oligoribonucleotides were provided (Fig. 5). Compounds **2e**, **2g**, **2h** and **2i** have individual interaction pattern implies that a change in the structure may result in the alteration of interaction pattern.

3. Conclusions

In a previous paper **2a–n** were prepared by following a 4-step-route in 22–33% total yields. In this paper **2a–n** were prepared by following a one-pot-preparation in 36–48% total yields. Thus the preparation of **2a–n** was improved. In vitro some of the present compounds were capable of inhibiting the proliferation of cancer cell lines at a nanomolar concentration. In the toxicology evaluation the healthy mice receiving up to a dose of 500 mg/kg of some of the present compounds neither gave neurotoxic response nor occurred death. In vivo even 0.01 mg/kg of **2h** and **2i** were still able to inhibit the tumor growth of the treated S180 mice. The fluorescence titration indicated that **2a–n** were able to interact with DNA. In the oligoribonucleotides based docking studies **2a–n** showed individual preferring interaction pattern. Combining the similar in vitro and in vivo anti-tumor activities of **2e**,**g**,**h**,**i** with their individual preferring interaction pattern it is demonstrated that they may gain their in vitro and in vivo anti-tumor action via individual interaction pattern.

4. Experimental section

4.1. Synthesis

4.1.1. General

The protected amino acids with L-configuration were purchased from Sigma Chemical Co. All the coupling and deprotective reactions were carried out under anhydrous conditions. Chromatography was performed on Qingdao silica gel H. The purities of the intermediates and the products were tested on TLC (Merck silica gel plates of type 60 F_{254}, 0.25 mm layer thickness) and HPLC (Waters, C_{18} column 4.6 × 150 mm), respectively. HPLC purities of 1,2,3,5,11,11a-hexahydro-3,3-dimethyl-1-oxo-6*H*-imidazo-[3′,4′:1,2]pyridin[3,4-*b*]indole-2-substituted acetates (**2a**–**n**) range from 98.0% to 98.9%. FAB-MS was determined by VG-ZAB-MS high resolution GC/MS/DS and HP ES-5989x. Optical rotations were determined with a Schmidt+Haensch Polartromic D instrument. The statistical analysis of all the biological date was carried out by use of ANOVA test with p <0.05 as significant cut-off.

4.1.2. 3*S*-1,2,3,4-Tetrahydro-β-carboline-3-carboxylic acid (1)

To a mixture of 5.0 g (24.5 mmol) of L-tryptophane, 25 mL of H_2SO_4 (1 mol/L) and 80 mL of water 8 mL of formaldehyde (36–38%) was added. The reaction mixture was stirred at room temperature for 2 h and adjusted to pH 6–7 with concentrated ammonia liquor. The mixture obtained was kept at 0 °C for 12 h and the formed precipitates were collected by filtration. After recrystallization 3.97 g (75%) of the title compound were obtained as a colorless powder. Mp 280–282 °C; ESI/MS (*m*/*z*) 217 $[M+H]^+$; IR (KBr): 3450, 3200, 3000, 2950, 2850, 1700, 1601, 1452, 1070, 900 cm^{-1}; ^1H NMR (BHSC-500, DMSO-d_6): δ = 10.99 (s, 1H), 9.89 (s, 1H), 7.30 (t, J = 7.5 Hz, 1H), 7.22 (t, J = 8.0 Hz, 1H), 7.01 (d, J = 8.0 Hz, 1H), 6.81 (d, J = 7.5 Hz, 1H), 4.01 (t, J = 4.8 Hz, 1H), 3.75 (dd, J = 10.5 Hz, J = 5.0 Hz, 1H), 3.64 (dd, J = 10.5 Hz, J = 2.4 Hz, 1H), 2.91 (d, J = 10.5 Hz, 2H), 2.86 (s, 1H).

4.1.3. General procedure for the preparation of benzyl 1,2,3,5,11,11a-hexahydro-3,3-dimethyl-1-oxo-6*H*-imidazo[3′,4′:1,2]pyridin[3,4-*b*]indole-2-substitutedacetate (2a–n)

(A) The suspension of 550 mg (2.5 mmol) of **1** in 10 mL of DMF and 0.8 mL of triethylamine was vigorously stirred at room temperature, to which 376 mg (2.6 mmol) of Boc-N_3 was added in 30 min. The reaction mixture was stirred at room temperature for 12 h and at 40 °C for 20 h and TLC ($CHCl_3$/CH_3OH, 5:1) indicated complete disappearance of **1**. The reaction mixture was cooled to 0 °C.

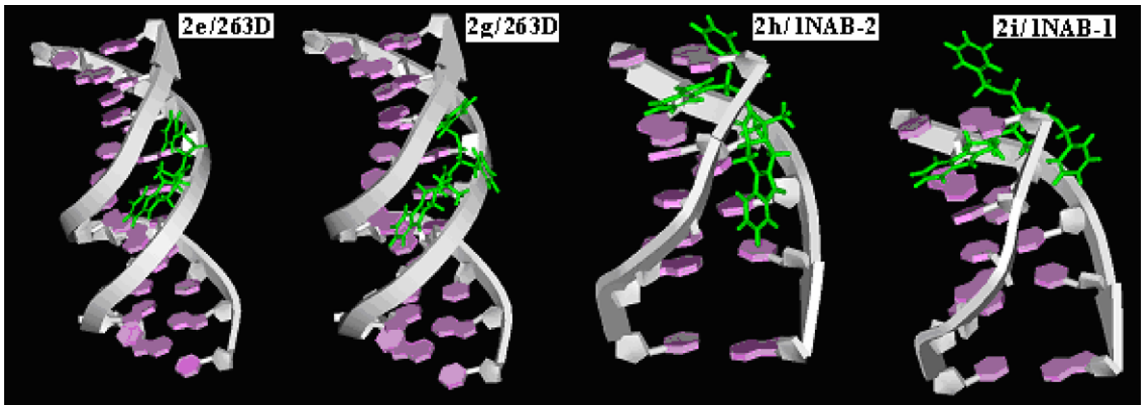

Figure 5. Stereoview of the docking complexes of **2e**/263D, **2g**/263D, **2h**/1NAB-2 and **2i**/1NAB-1.

(B) To this reaction mixture 10 mL of anhydrous THF and 377 mg (2.8 mmol) of HOBt were added, after 10 min 556 mg (2.7 mmol) of DCC were added, after another 10 min a solution of 2.6 mmol of amino acid benzylester in 3 mL of anhydrous THF were then added. The reaction mixture was stirred at 0 °C for 2 h and at room temperature for 8 h.

(C) On evaporation the residue was dissolved in 5 mL of anhydrous ethyl acetate and the solution was cooled to 0 °C and filtrated. To the filtrate 16 mL of hydrogen chloride/ethyl acetate (4 N) were added dropwise. The reaction solution was stirred at 0 °C for 90 min and evaporated under reduced pressure. The residue obtained was dissolved in 50 mL of methanol and 10 mL of acetone. With triethylamine the reaction solution was adjusted to pH 9, at room temperature and in dark stirred for 240 h, and TLC ($CHCl_3/CH_3OH$, 10/1) indicated the complete disappearance of *N*-[(3*S*)-*N*-1,2,3,4-tetrahydro-β-carboline-3-carbonyl]-L-amino acid benzylester. On evaporation the residue was dissolved in 5 mL of methanol to give **2a–n** as crystals (Analytical data see Supplementary data).

4.2. Bioassays

4.2.1. In vitro cytotoxic assay

All stock cultures were grown in T-25 flasks. Freshly trypsinizer cell suspensions were seeded in 96-well microtiter plates at densities of 5000 cells per well with **2a–n** added from DMSO-diluted stock. After 3 days in culture, attached cells were fixed with cold 10% trichloroacetic acid and then stained with 0.4% sulforhodamine B. The absorbance at 562 nm was measured using a microplate reader after solubilizing the bound dye. The mean IC_{50} is the concentration of **2a–n** that reduces cell growth by 50% under the experimental conditions and is the average from at least three independent determinations that were reproducible and statistically significant. The following human tumor cell lines were used in the assay: A549, PC-3, KB, KB-VIN, and MCF-7. All cell lines were obtained either from the Lineberger Cancer Center (UNC-CH) or from ATCC (Rockvile, MD) and were cultured in RPMI-1640 medium supplemented with 25 mM HEPES, 0.25% sodium bicarbonate, 10% fetal bovine serum, and 100 μg/mL kanamycin.

4.2.2. In vivo anti-tumor assay

Male ICR mice, purchased from Peking University Health Science Center, were maintained at 21 °C with a natural day/night cycle in a conventional animal colony. The mice were 10–12 weeks old at the beginning of the experiments. S180 ascites tumor cells were used to form solid tumors after subcutaneously injection. For initiation of subcutaneous tumors the cells were obtained as an ascitic form from the tumor-bearing mice, which were serially transplanted once per week. Subcutaneous tumors were implanted by injecting 0.2 mL of 0.9% saline containing 1×10^7 viable tumor cells under the skin on the right armpit. Twenty-four hours after implantation, the mice (twelve per group) were randomly divided into experimental groups. Doxorubicin is well known as an intercalating agent. To clarify the validity of the mouse model and to have a similar action mechanism doxorubicin was selected as the positive control. The mice of the positive control group were given a daily ip injection of 1.0 mg/kg of doxorubicin in 0.2 mL of 0.9% saline for seven consecutive days. The mice of the negative control group were given a daily ip injection of 0.2 mL of 0.9% saline for seven consecutive days. The mice of the treatment groups were given a daily ip injection of 1.0 mg/kg of **2a–n** in 0.2 mL of 0.9% saline for seven consecutive days. The weights of animals were recorded everyday. Twenty-four hours after the last administration, all mice were weighed, sacrificed by diethyl ether anesthesia and dissected to immediately obtain and weigh the tumor and spleen samples. The inhibition ratio was calculated based on inhibition ratio (%) = $[(A - B)/A] \times 100$, wherein A is average tumor weight of the negative control, and B is that of the treatment group.

4.2.3. Acute toxicities assay

ICR mice, purchased from Peking University Health Science Center, were maintained at 21 °C with a natural day/night cycle in a conventional animal colony. The mice were 10–12 weeks old at the beginning of the experiments. The sterile food and water were provided according to institutional guidelines. Prior to each experiment, mice were fastened overnight and allowed free access to water. The mice were given an ip injection of 10, 100 or 500 mg/kg of **2e,g,h,i** in 0.2 mL of 0.9% saline. Each group contained 12 mice (six males and six females). After the administration the mice were monitored continuously for up to 7 days to observe any abnormal behavior or death. All animals were sacrificed on the seventh day and checked macroscopically for possible damage to the heart, liver, and kidneys. LD50 values were calculated graphically. The study described herein was performed according to a protocol reviewed and approved by the ethics committee of Capital Medical University. The committee ensures that the welfare of the animals is maintained in accordance to the requirements of the Animal Welfare Act and according to the Guide for Care and Use of Laboratory Animals.

4.3. Determination of the retention time and thus Log *K* of 2a–n

Benzyl 1,2,3,5,11,11a-Hexahydro-3,3-dimethyl-1-oxo-6*H*-imidazo[3′,4′:1,2]pyridin[3,4-*b*]indole-2-substitutedacetates **2a–n** were dissolved in aqueous methanol (50%) to prepare sample solutions of 10 μM. The HPLC analysis was carried out on Agilent 1100 series, the column was a reversed-phase C18 column (Agilent 1100 series, Agilent Zorbax Extend-C18, 4.6 × 15 mm, 5 μm). After 20 μL of the sample (10^{-5} M) was loaded, the column was eluted with a solution consisted of 0.7 CH_3OH/0.3 H_2O as the mobile phase for 40 min. The flow rate was 1 mL/min. The peak of **2a–n** in the sample was monitored with UV detector at 254.8 nm and the retention time (t_R) corresponding to its peak was recorded. With the same HPLC conditions the retention time of acetone peak was recorded as t_0. In order to offset the influence of the solvent on the appearance time of the peak of **2a–n**, the appearance time of acetone peak (t_0, 1.591 min) was used as a control. As an alternative representation of t_R, Log K was defined based on the equation Log K = Log$[(t_R - t_0)/t_0]$.

Acknowledgements

This work was finished in Beijing Area Major Laboratory of Peptide and Small Molecular Drugs, supported by the National Natural Scientific Foundation of China (30801426, 30901843) Special Project (2008ZX09401-002) of China and PHR (IHLB, KZ200810025010) and PHR (IHLB, KZ200810025010 & KZ200910025004).

Supplementary data

Supplementary data (analytical data (^1H, ^{13}C NMR, MS, etc.) for compounds **2a–n**) associated with this article can be found, in the online version, at doi:10.1016/j.bmc.2010.01.038.

References and notes

1. Jiménez, J.; Riverón-Negrete, L.; Abdullaev, F.; Espinosa-Aguirre, J.; Rodríguez-Arnaiz, R. *Exp. Toxicol. Pathol.* **2008**, *60*, 381.
2. Tu, L. C.; Chen, C.-S.; Hsiao, I.-C.; Chern, J.-W.; Lin, C.-H.; Shen, Y.-C.; Yeh, S. F. *Chem. Biol.* **2005**, *12*, 1317.

3. Xu, Y.; Afonso, C.; Gimbert, Y.; Fournier, F.; Dong, X.; Wen, R.; Tabet, J.-C. *Int. J. Mass Spectrom.* **2009**, *286*, 43.
4. Laronze, M.; Boisbrun, M.; Léonce, S.; Pfeiffer, B.; Renard, P.; Lozach, O.; Meijer, L.; Lansiaux, A.; Bailly, C.; Sapi, J.; Laronze, J.-Y. *Bioorg. Med. Chem.* **2005**, *13*, 2263.
5. Beauchard, A.; Jaunet, A.; Murillo, L.; Baldeyrou, B.; Lansiaux, A.; Chérouvrier, J.; Domon, L.; Picot, L.; Bailly, C.; Besson, T.; Thiéry, V. *Eur. J. Med. Chem.* **2009**, *44*, 3858.
6. Napper, A. D.; Hixon, J.; McDonagh, T.; Keavey, K.; Pons, J.-F.; Barker, J.; Yau, W. T.; Amouzegh, P.; Flegg, A.; Hamelin, E.; Thomas, R. J.; Kates, M.; Jones, S.; Navia, M. A.; Saunders, J. O.; DiStefano, P. S.; Curtis, R. *J. Med. Chem.* **2005**, *48*, 8045.
7. Boeira, J. M.; Viana, A. F.; Picada, J. N.; Henriques, J. A. P. *Mutat. Res.* **2002**, *500*, 39.
8. Mansoor, T. A.; Ramalho, R. M.; Mulhovo, S.; Rodrigues, C. M. P.; Ferreira, M. J. U. *Bioorg. Med. Chem. Lett.* **2009**, *19*, 4255.
9. Behforouz, M.; Cai, W.; Mohammadi, F.; Stocksdale, M. G.; Gu, Z.; Ahmadian, M.; Baty, D. E.; Etling, M. R.; Al-Anzi, C. H.; Swiftney, T. M.; Tanzer, L. R.; Merriman, R. L.; Behforouz, N. C. *Bioorg. Med. Chem.* **2007**, *15*, 495.
10. Takikawa, O. *Int. Congress Series* **2007**, *1304*, 290.
11. Pouilhès, A.; Kouklovsky, C.; Langlois, Y.; Baltaze, J.-P.; Vispé, S.; Annereau, J.-P.; Barret, J.-M.; Kruczynski, A.; Bailly, C. *Bioorg. Med. Chem. Lett.* **2008**, *18*, 1212.
12. Deveau, A. M.; Labroli, M. A.; Dieckhaus, C. M.; Barthen, M. T.; Smith, K. S.; Macdonald, T. L. *Bioorg. Med. Chem. Lett.* **2001**, *11*, 1251.
13. Arzel, E.; Rocca, P.; Grellier, P.; Labae, M.; Frappier, F.; Guéritte, F.; Gaspard, C.; Marsais, F.; Godard, A.; Quéguiner, G. *J. Med. Chem.* **2001**, *44*, 949.
14. Jenkins, P. R.; Wilson, J.; Emmerson, D.; Garcia, M. D.; Smith, M. R.; Gray, S. J.; Britton, R. G.; Mahale, S.; Chaudhuri, B. *Bioorg. Med. Chem.* **2008**, *16*, 7728.
15. Song, Y.; Kesuma, D.; Wang, J.; Deng, Y.; Duan, J.; Wang, J. H.; Qia, R. Z. *Biochem. Biophys. Res. Commun.* **2004**, *317*, 128.
16. Hurley, L. H. *Nat. Rev. Cancer* **2002**, *2*, 188.
17. Martinez, R.; Chacon-Garcia, L. *Curr. Med. Chem.* **2005**, *12*, 127.
18. Zhao, M.; Bi, L.; Wang, W.; Wang, C.; Baudy-Floc'h, M.; Ju, J.; Peng, S. *Bioorg. Med. Chem.* **2006**, *14*, 6998.
19. Li, N.; Ma, Y.; Yang, C.; Guo, L. P.; Yang, X. R. *Biophys. Chem.* **2005**, *116*, 199.
20. Wu, J.; Zhao, M.; Qian, K.; Lee, K.-H.; Morris-Natschke, S.; Peng, S. *Eur. J. Med. Chem.* **2009**, *44*, 4153.
21. Wu, J.; Cui, G.; Zhao, M.; Cui, C.; Peng, S. *Mol. Biosyst.* **2007**, *3*, 855.
22. Liu, J.; Cui, G.; Zhao, M.; Cui, C.; Ju, J.; Peng, S. *Bioorg. Med. Chem.* **2007**, *15*, 7773.
23. Zhao, M.; Li, Z.; Wu, Y.; Wang, C.; Zhang, Z.; Peng, S. *Eur. J. Med. Chem.* **2007**, *42*, 955.
24. Kaizerman, J. A.; Gross, M. I.; Ge, Y.; White, S.; Hu, W.; Duan, J.-X.; Baird, E. E.; Johnson, K. W.; Tanaka, R. D.; Moser, H. E.; Bürli, R. W. *J. Med. Chem.* **2003**, *46*, 3914.
25. Opitz, A.; Roemer, E.; Haas, W.; Görls, H.; Werner, W.; Gräfe, U. *Tetrahedron* **2000**, *56*, 5147.
26. Queiroz, R. P.; Castanheir, M. S. E.; Lopes, C. T. T.; Cruz, K. Y.; Kirsch, G. *J. Photochem. Photobiol., A* **2007**, *190*, 45.
27. Sobhani, A. M.; Amini, S. R.; Tyndall, J. D. A.; Azizi, E.; Daneshtalab, M.; Khalaj, A. *J. Mol. Graphics Modell.* **2006**, *25*, 459.
28. Clark, G. R.; Gray, E. J.; Neidle, S.; Li, Y.-H.; Leupin, W. *Biochemistry* **1996**, *35*, 13745.